Rev.Adv.Mater.Sci. 22(2009) 21-38

CONTRIBUTIONS TO THE MODELLING OF THE MILLING PROCESS IN A PLANETARY BALL MILL

Gy. Kakuk[1], I. Zsoldos[1], Á. Csanády[2] and I. Oldal[1]

[1]Szent Istvan University, Faculty of Mechanical Engineering, H-2103, Páter Karoly str. 1, Gödöllő, Hungary
[2]Bay Zoltán Foundation, Institute of Materials Science and Technology, H-1116, Fehervari str. 130, Budapest, Hungary

Received: February 04, 2009

Abstract. Further improving the previous models describing the operation of planetary ball mills, the study determines the *impact energy* transmitted towards the material during the milling and the *milling power*. It points out relationship between the ratio between the angular velocity of the sun disk and the vials, and the geometrical parameters of the mill. By exploring the relationship between the model created for the milling process taking place in the planetary ball mill and the milling parameters depending on the mill, and using the calculations executed, data more authentic than previous ones can be obtained *on the energy transferred to the mill product during the milling process,* and *on the efficiency of milling*. This information provides more plannable mechanical milling for researchers decomposing materials in planetary mills, and for specialists dealing with the improvement and application of these technologies.

1. INTRODUCTION

Nowadays, there are several possible solutions for producing nano-structure materials using conventional and/or newly developed technologies of material science [1,2]. During these processes the size, structure, composition, and morphological characteristics of “grains” and/or “phases” can be altered with the aimed selection of technological parameters. Possible ways of production include mechanical milling having been applied for decades in the production of powder materials [3-5]. The improvement results of different type mills (e.g. the possibility of higher energy input) have made it possible by now to produce nano-crystalline powders by mechanical milling. However, it is inevitable to have adjustability more accurate then before, for purposive milling and the quality insurance of products intended to be produced by milling [6,7].

During the milling process (Fig. 1.) carried out in the planetary mill, the impact velocity and the angle of impact has a significant effect on the energy transferred to the powder particles to be milled by the flying ball. Consequently, the movement and impact of the balls are important factors, on the inspection of which thorough mathematical studies have been carried out [9-11].

According to Lü and Lai [12] the greater is the angular velocity of the sun disk, the greater is the increase in the impact velocity as the detachment velocity of the balls increases and the flying time shortens. This impact velocity is an important parameter, which determines what energy acts upon the powder particles during the mechanical milling.

Besides and before Lü and Lai, several authors and studies had already dealt with determining the energy transferred by the balls to the material to be milled. The study of Burgio et al. [13] has been considered initial basis for many when determining the impact velocity of the ball and the energy transferred to the powder. Analyzing the above

Corresponding author: Gy. Kakuk, e-mail: kakuk.gyula@gek.szie.hu

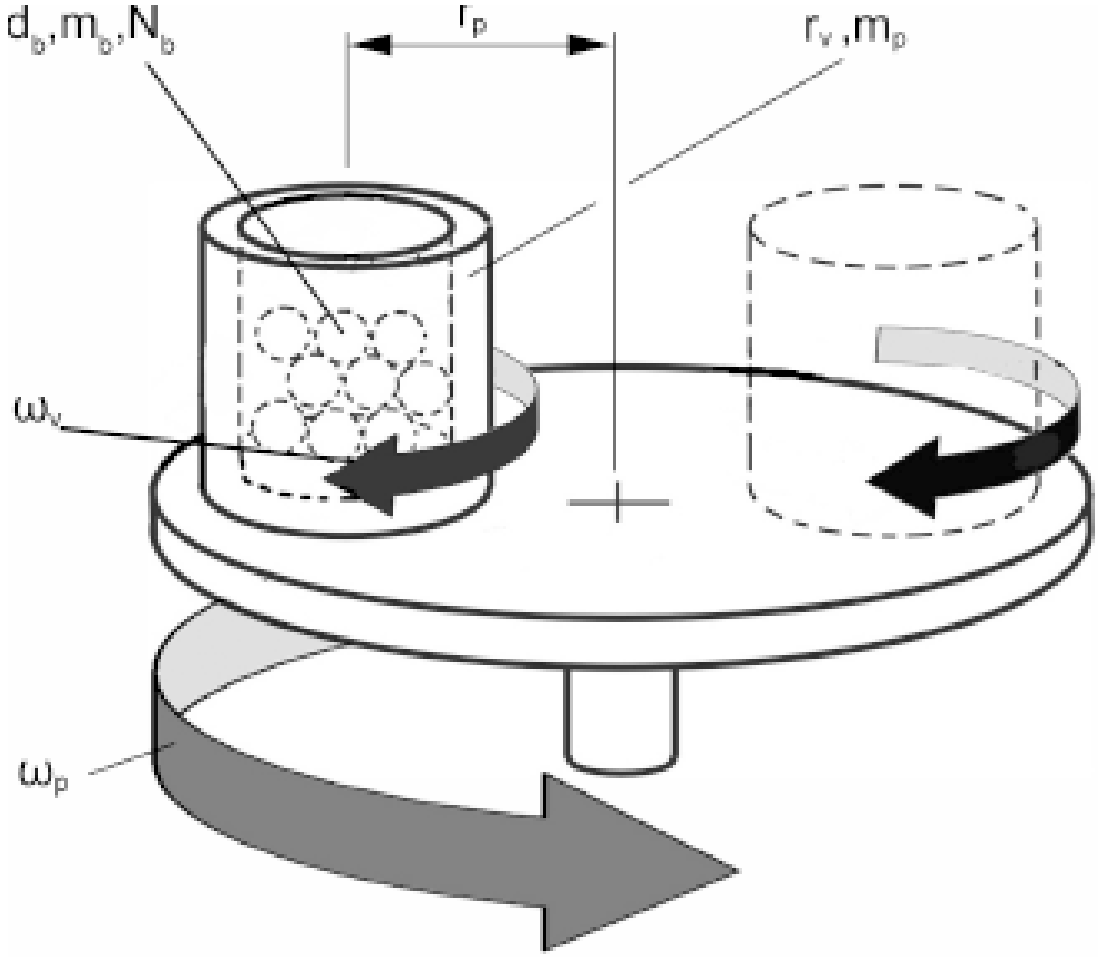

Fig. 1. Process parameters of the planetary ball mill [8]. d_b: the diameter of the balls, m_b: the mass of the balls, N_b: the number of the balls, r_p: the distance between the rotational axes, r_v: the radius of the vial, m_p: the mass of the powder, ω_v: the rotational speed of the vial, ω_p: the rotational speed of the sun disk.

studies it can be stated that when determining the detachment angle and the detachment velocity they do not take into consideration forces resulting from *relative movements* (e.g. Coriolis force). Impact energy is described as the difference between the kinetic energy calculated for the moment of detachment of the ball and the velocityof the ball after the impact. No information is given on determining the location of the impact. Although, they give data of exact (measured) speed and detachment angle for a certain setup of mill type Pulverisette P5 and different ball sizes, but they provide no calculated impact energy.

P. Le Brun et al. [9] published another relationship on determining the detachment angle of the milling ball, and they highlight the importance of the speed rate (ratio) between the sun disk and the vial, which influences the trajectory of the balls, and even the amplitude and ratio of the impact and friction energy which can be transferred to the material to be milled. In their study, Abdellaoui and Gaffet [14] present the change in impact energy and power related to the angular velocity of the sun disk primarily in connection with planetary mills types G5 and G7 (but also for other milling devices), however, they do not give their calculation relationships. In another study [11] relying upon the work of the above mentioned Burgio et al. [13] they present calculation correlations for determining the impact energy, but no information is found on the location of the impact, furthermore, they do not take forces resulting from relative movements into consideration either in their calculations. Magini et al. [15,16] give a simplified correlation for determin-

ing impact energy in their study, and they focus on inspecting the collision between the ball and the material to be milled. Iasonna and co. Magini [17] in one of their studies examined energy transfer and power consumption during the milling process. They measured electric and mechanical power consumption on a Fritsch P5 milling device. During milling Fe-Zr powder they examined the influence of the number and size of balls, and that of the quantity of powder filled-in on the power consumption. Rojac et al. [18] prepared the so-called milling map of a $NaNbO_3$ ceramic-oxide system. Every point of the milling map indicates a certain state of the mechanochemical reaction. From the milling map the experimental states, e.g. milling parameters can be determined in order to achieve the intended end-product. For the calculation of impact energy values used for the milling maps, the equations of Burgio were used with minor alterations.

Several researchers have already dealt with modelling processes taking place in the planetary ball mill (Fritsch P4) used during our work, however, literature dealing with the relationship between the milling parameters regulating the process and the energy transferred to the material to be milled is incomplete. Taking this fact into consideration, it is reasonable to further clarify processes taking place in the planetary ball mill, and a more accurate exploration of the influence of some important milling parameters.

2. KINETIC MODELLING OF A PLANETARY BALL MILL

The description of forces acting on the milling ball in the planetary ball mill is based on the study of Lü and Lai [12]. After a verification the calculation mentioned can be used as an initial point for the model intended to be established. A part of this description should be outlayed in appendix point A1 and A2 in order to understand the whole model.

From chapter 2.1. the further construction details of the model introduced by Lü and Lai will be described. Our contributions concerning the kinetic modelling of the mechanical milling process of the planetary ball mill was started with the following statements and simplifying assumptions:

(a) the milling ball can detach from the wall of the vial, when the force acting upon it, pointing towards the radius of the vial is zero,
(b) the new junction point of the ball and the vial acts as a point of impact, disregarding the elastic impact of the ball,
(c) there is no relative movement (sliding) between the ball and the wall of the vial before the point of detachment,
(d) the resistance of the medium within the vial is neglected,
(e) any rotation of the ball is disregarded.

Modelling steps are as follows:

- Description of motion and force conditions
- Determining the detachment angle
- Determining the detachment velocity
- Determining the impact point
- Determining the impact velocity
- Determining the impact energy and power
- Calculating planetary ball mill working curves.

2.1. The influence of the ratio (*i*) on the angle of detachment and on the ball trajectory

The detachment and impact positions depend on the size of the vial (r_v), the position of the vial on the sun disk (r_p), and the rate of the rotational speed, that is the ratio (i). When r_v and r_p are fixed, detachment depends on only i, therefore it seems to be reasonable to determine those ratio values, under, between, and above which the milling ball runs on a different trajectory.

The determination of the limits of the ratio was started from relationship (A.18) (see appendix A2.) Inspecting the relationship it can easily be understood that the angle of detachment can only be interpreted between +1 and -1, that is the solution of the inequations

$$-\frac{r_v}{r_p}\cdot(1-i)^2 \geq -1, \quad \text{and} \tag{2.1}$$

$$-\frac{r_v}{r_p}\cdot(1-i)^2 \leq 1, \tag{2.2}$$

provide the values of i_{limit} and $i_{critical}$ by fixed geometrical parameters (r_p, r_v).

Inequation (2.2) is valid in case of any arbitrarily chosen speed ratio and geometrical characteristics due to the negative sign before the fraction r_v/r_p.

Results of the inequation (2.1) provide the limit values of the ratio, which will be as follows without the steps of deduction:

$$i_{limit} = 1-\sqrt{\frac{r_p}{r_v}} \leq i \leq 1+\sqrt{\frac{r_p}{r_v}} = i_{critical}. \tag{2.3}$$

From relationships (A.17) (see appendix A2.) and (2.3) it can be stated that in case of using the con-

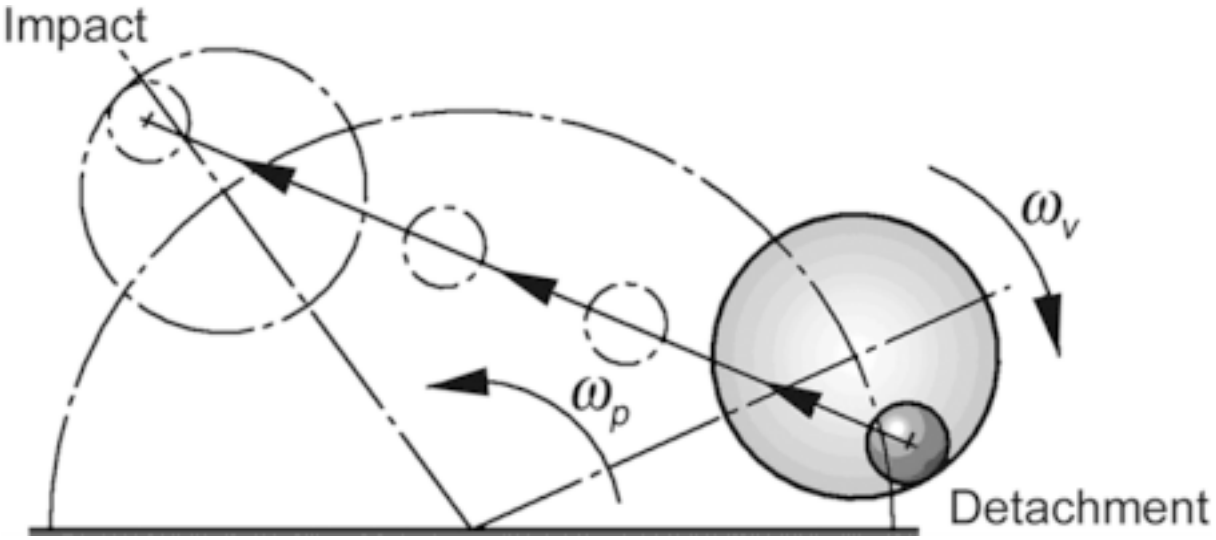

Fig. 2. Movement of the ball after detachment, when $i_{limit} \le i \le i_{critical}$.

struction of a given mill (r_p) and a given vial (r_v), the rotational speed of the sun disk (ω_p) and the vials (ω_v) should be set in a way that the condition (2.3) is met, in order to achieve the greatest possible impact energy and the best possible milling power, as the ball detaches from the wall of the vial at this point. If this condition is met, that is $i_{limit} \le i \le i_{critical}$, then milling will be implemented according to the impact and friction method, when the kinetic energy transmitted by the milling balls to the powder is the greatest possible.

As a function of i_{limit} and $i_{critical}$, the trajectory of the balls determines three operational modes, the existence of which has already been verified by experiments of Brun et al. [9]:
- chaotic mode *(*if $i < i_{limit}$ *)*
- impact and friction mode *(*if $i_{limit} \le i \le i_{critical}$*)*
- pure friction mode *(*if $i > i_{critical}$*)*.

2.2. Impact and friction mode

In this mode, as indicated by Fig. 2, the trajectory of the ball is described very well by the principles of dynamics. Energy can be divided into two components at the moment of the impact. Namely, to the normal component, which results in the increase of the effective impact energy transferred to the powder particles, and to the tangential component, which may occur as friction energy.

The above described behaviour of the milling balls is the most advantageous for carrying out effective milling, therefore it is reasonable to inspect, what set of rotational speed values is the condition $i_{limit} \le i \le i_{critical}$ met with the given geometrical parameters.

2.3. Determining the detachment velocity (v_d)

In order to be able to determine the energy released during the impact of the ball after the detachment, it is necessary to know the speed and direction of the ball. After determining the angle of detachment (A.18), see appendix A2, the absolute point '*A*' (X_d,Y_d) of detachment, and the two components of the detachment velocity, v_{dx} and v_{dy} can be determined in directions *X* and *Y*, on suppositon that the ball and the vial move together at the moment of detachment.

Detachment velocity (v_d) at point '*A*' is given by the sum of the peripheral velocity of the sun disk (v_{dp}) and the peripheral velocity of the vial (v_{dv}). Based on the indications of Fig. 3., the peripheral velocity resulting from the rotation of the vial and its *X* and *Y* direction components are:

$$v_{dv} = r_v \cdot \omega_v, \tag{2.4}$$

$$v_{dvx} = -\left[v_{dv} \cdot \cos\left(\frac{\pi}{2} - (\varphi_d - \Omega_d) \right) \right] = -\left[r_v \cdot \omega_v \cdot \sin(\varphi_d - \Omega_d) \right], \tag{2.5}$$

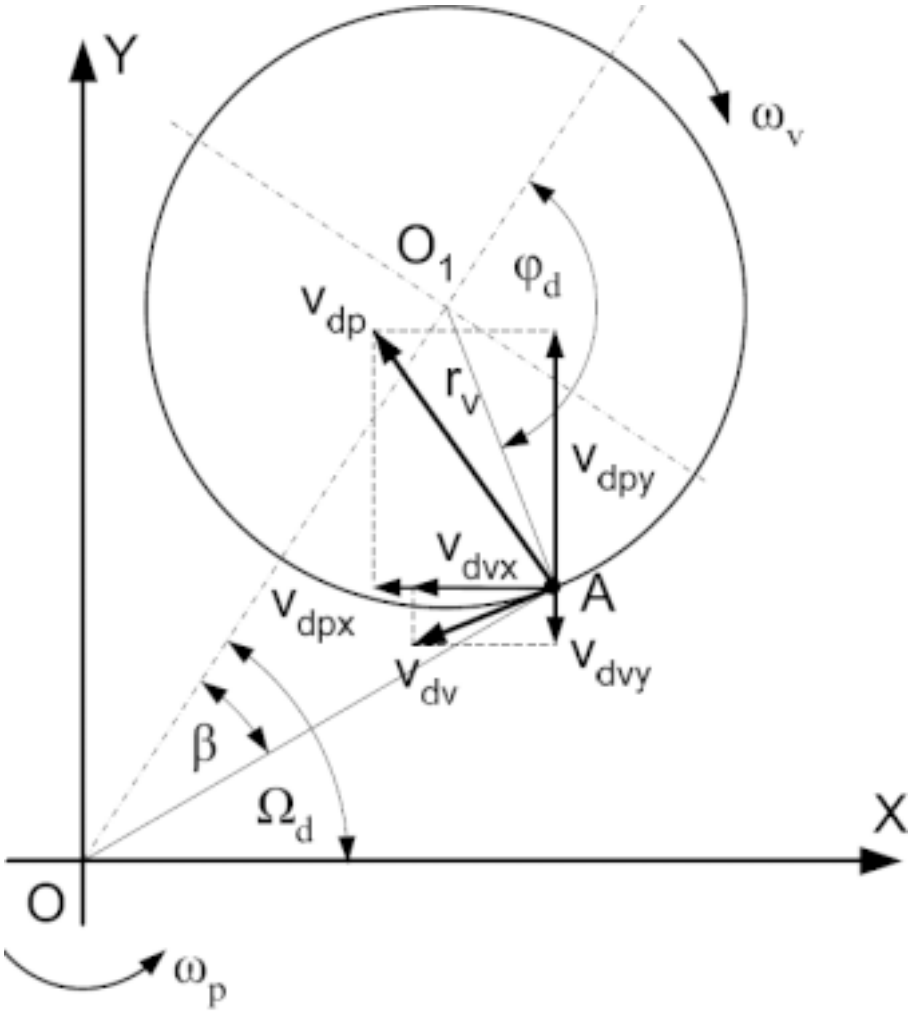

Fig. 3. Interpretation of the detachment velocity.

$$v_{dvy} = -\left[v_{dv} \cdot \sin\left(\frac{\pi}{2} - \left(\varphi_d - \Omega_d\right)\right)\right] = -\left[r_v \cdot \omega_v \cdot \cos\left(\varphi_d - \Omega_d\right)\right]. \tag{2.6}$$

Similarly, the *X* and *Y* direction components resulting from the peripheral velocity of the sun disk can be stated:

$$v_{dp} = \overline{OA} \cdot \omega_p . \tag{2.7}$$

where *OA* is the distance between the centre of the sun disk and the detachment point 'A':

$$\overline{OA} = \sqrt{r_p^2 + r_v^2 - 2 \cdot r_p \cdot r_v \cdot \cos\left(\pi - \varphi_d\right)}, \tag{2.8}$$

$$v_{dpx} = -\left[v_{dp} \cdot \cos\left(\frac{\pi}{2} - \left(\Omega_d - \beta\right)\right)\right] = -\left[\overline{OA} \cdot \omega_p \cdot \sin\left(\Omega_d - \beta\right)\right], \tag{2.9}$$

$$v_{dpy} = v_{dp} \cdot \sin\left(\frac{\pi}{2} - \left(\Omega_d - \beta\right)\right) = \overline{OA} \cdot \omega_p \cdot \cos\left(\Omega_d - \beta\right). \tag{2.10}$$

Based on the above the detachment velocity and its *X* and *Y* direction projections can be stated as:

$$v_{dx} = v_{dvx} + v_{dpx}, \tag{2.11}$$

$$v_{dx} = -r_v \cdot \omega_v \cdot \sin\left(\varphi_d - \Omega_d\right) - \overline{OA} \cdot \omega_p \cdot \sin\left(\Omega_d - \beta\right), \tag{2.12}$$

$$v_{dy} = v_{dvy} + v_{dpy}, \tag{2.13}$$

$$v_{dy} = -r_v \cdot \omega_v \cdot \cos\left(\varphi_d - \Omega_d\right) + \overline{OA} \cdot \omega_p \cdot \cos\left(\Omega_d - \beta\right). \tag{2.14}$$

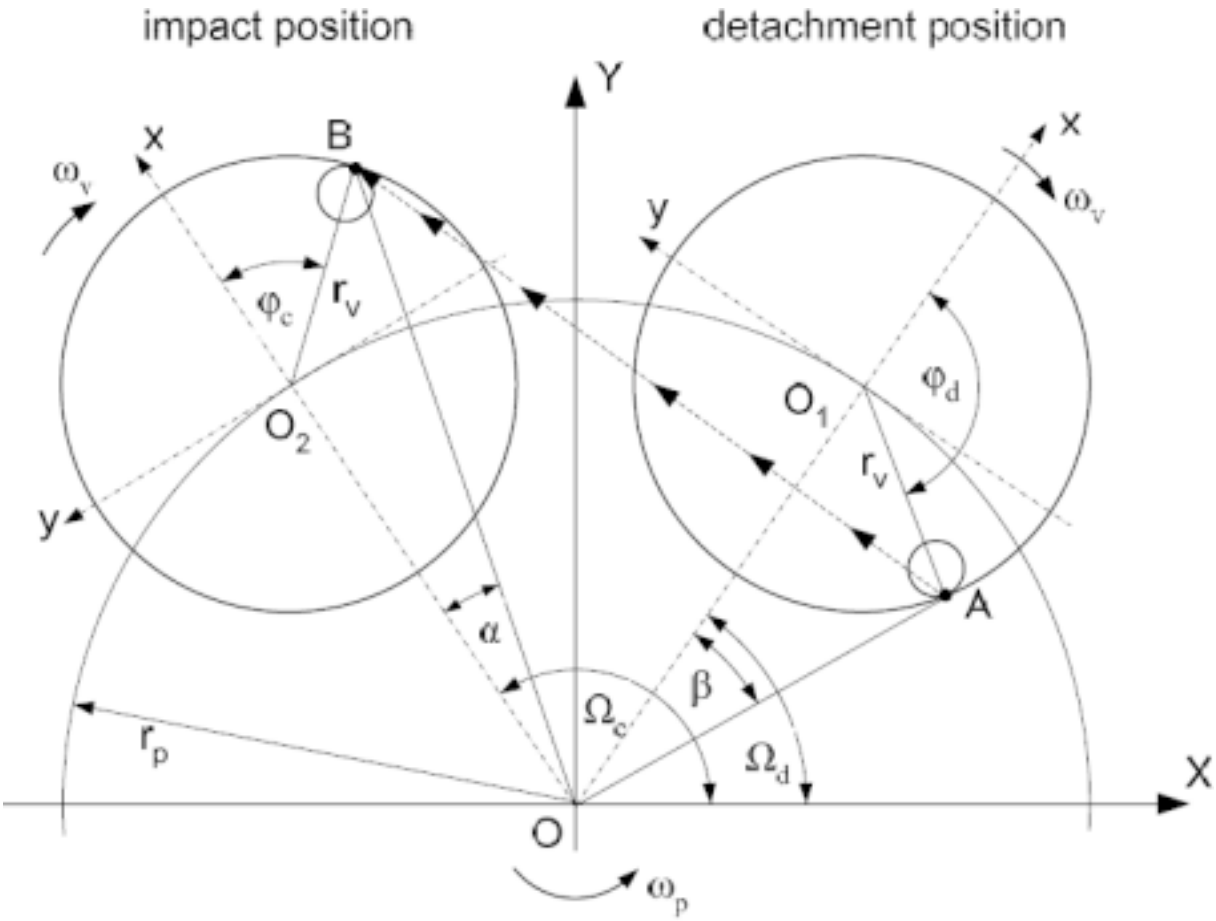

Fig. 4. Motion of the ball from the detachment to the impact.

Based on the relations (2.12. and 2.14.) the detachment velocity can be determined:

$$v_d = \sqrt{v_{dx}^2 + v_{dy}^2}. \qquad (2.15)$$

3. KINETIC ENERGY OF THE MILLING BALL AT THE MOMENT OF IMPACT

From this step on (including detachment velocity determined above) the model has been further built using our own algorithm. The works of others in known and available literature sources could not be followed as:

- they do not provide calculations concerning the determination of the impact point, despite the fact that this is one of the most difficult and most definitive steps of the model,
- in models related to planetary ball mills the size of the ball is neglected, i.e. it is considered to be point-like. This simplification is not acceptable. Fig. 5. shows that the angle φ_c belonging to the real impact point (*B*) may even be a multiple of the value, which would be determined in case of a point-like ball (point *B*', angle φ_c').

The calculation steps of the location of impact is given in details in this chapter in a way that even the dimensions of the ball are taken into account.

In order to determine the useful kinetic energy of the ball, the absolute velocity of the point of impact should be known. The difference between the velocity calculated in the impact point and the detachment velocity gives the relative velocity of the ball and the vial, i.e. the actual impact velocity. The projection of this velocity on the radius direction of the vial will be the velocity component, which is useful from the aspect of milling, so it should be taken into account when determining kinetic energy.

As the wall detaches from the wall of the vial, it is supposed that it will move straight and even with its detachment velocity. Kinetics of rigid bodies will be applied for the description of the free motion of

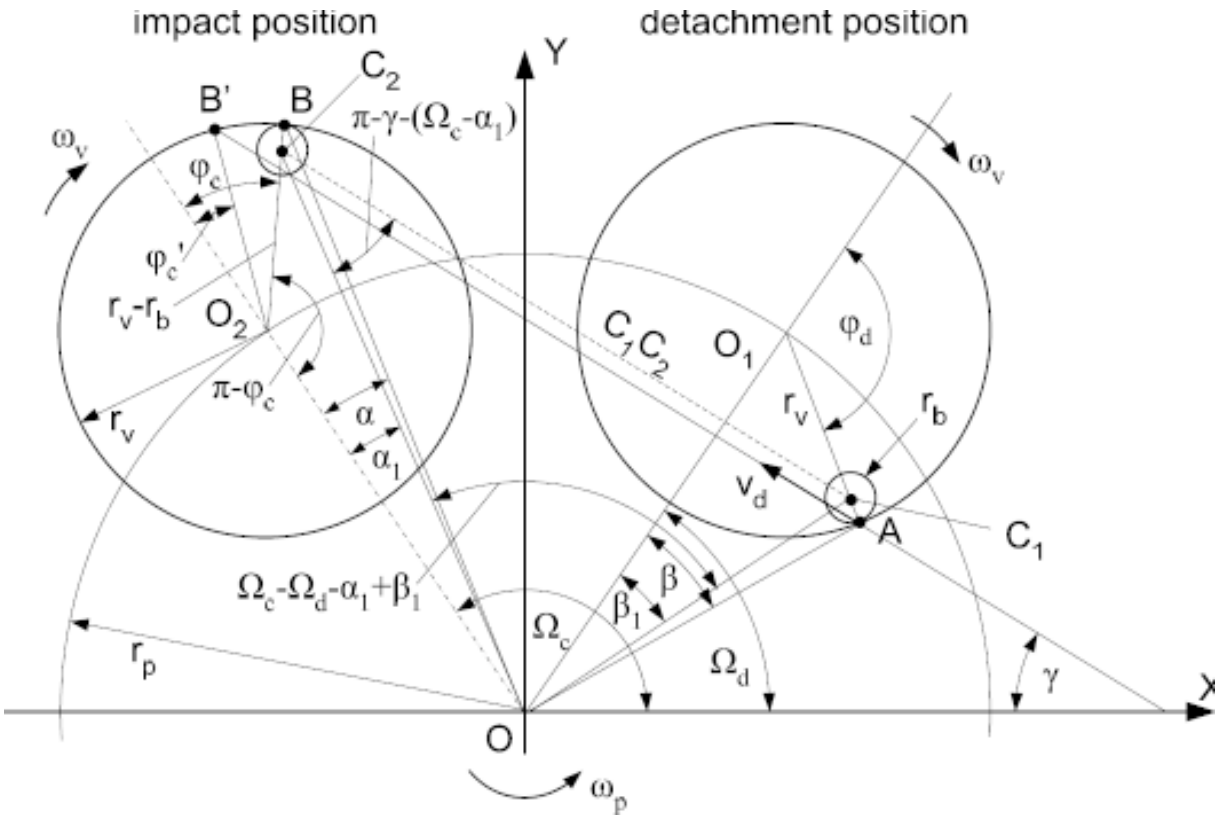

Fig. 5. Geometrical conditions of the impact of the ball.

the ball, until it meets the vial again. Fig. 4. demonstrates the motion of the ball from the detachment to the impact, where points '*A*' and '*B*' indicate the location of detachment and impact.

Exact knowledge of point 'B', that is the point of impact is essential in order to determine absolute velocity values there. For this, it needs to be determined, by what vial angle position (Ω_c) and related to the vial by what angle value (φ_c) does the ball impact by fixed sun disk (ω_p) – and vial (ω_v) rotary speed, and in case of the already known detachment velocity. The absolute velocity of the impact point is determined in an indirect way, which is to be introduced below.

3.1. Determining the parameters of the impact point

In order to determine the point of impact from the principles of the ball and vial motion the geometrical characteristics of the construction were used initially. Take a look at Fig. 5., which demonstrates the geometrical conditions of the ball impact.

From the aspect of the point of impact it is true concerning the relationship between the motion of the ball and the motion of the vial that during the time the ball reaches the point of impact starting with the detachment velocity (v_d) from the moment of detachment, the vial carries out Ω_c-Ω_d rotation with angular velocity ω_p around point "*O*". The relationship is:

$$\frac{\overline{C_1C_2}}{v_d} = \frac{\Omega_c - \Omega_d}{\omega_p}. \tag{3.1}$$

Since distance C_1C_2 and angle Ω_c are both unknown, above this the knowledge of angle φ_c is also necessary, further relationships are to be found. Based on Fig. 5. the geometrical principles concerning the triangle OC_2O_2 are as follows:

$$\frac{\sin\alpha_1}{\sin(\varphi_c - \alpha_1)} = \frac{r_v - r_b}{r_p}, \tag{3.2}$$

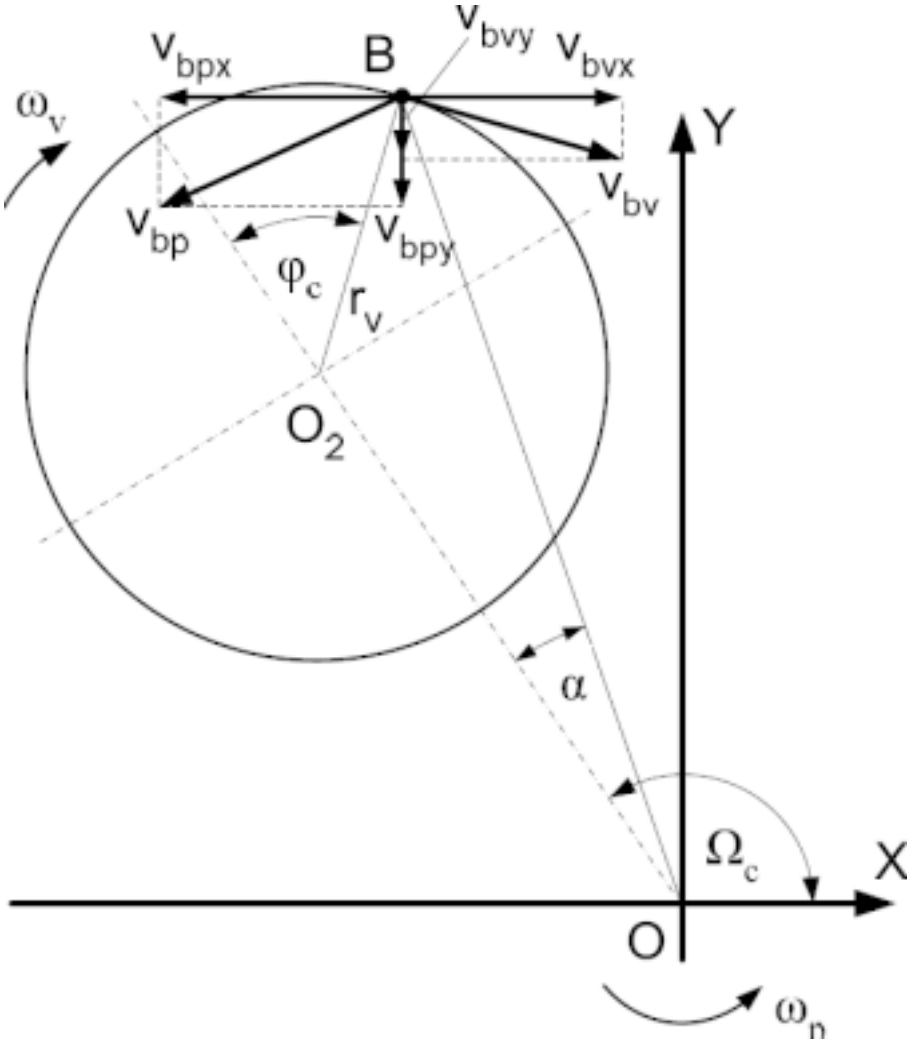

Fig. 6. Interpreting the velocity of the point of impact.

$$\overline{OC_2}^2 = r_p^2 + (r_v - r_b)^2 - 2 \cdot r_p \cdot (r_v - r_b) \cdot \cos(\pi - \varphi_c). \quad (3.3)$$

Also based on Fig. 5, the following relationships are true in case of triangleOC_1C_2:

$$\frac{\sin(\pi - \gamma - (\Omega_c \pm \alpha_1))}{\sin(\Omega_c - \Omega_d \pm \alpha_1 + \beta_1)} = \frac{\overline{OC_1}}{\overline{C_1C_2}}, \quad (3.4)$$

$$\overline{C_1C_2}^2 = \overline{OC_1}^2 + \overline{OC_2}^2 - 2 \cdot \overline{OC_1} \cdot \overline{OC_2} \cdot \cos(\Omega_c - \Omega_d \pm \alpha_1 + \beta_1). \quad (3.5)$$

Despite the fact that these are basic mathematical and physical relationships, the relationships (3.1-3.5) together form a non-linear system of equations with five unkowns, in which the unknown parameters are the angle of impact (φ_c), the angle position of the vial at the moment of impact (Ω_c), the distance of the ball centre from the axis of rotation of the sun disk (OC_2) and from the point of detachment (C_1C_2), and the angle (α_1) between OC_2 and OO_2. The determination of parameters 'φ_c' and 'Ω_c' are directly, while the above mentioned other parameters are only indirectly necessary for determining the absolute velocity of the point of impact. Finding the solution for the problem is further aggravated by the fact that if the point of impact is to the right or to the left from OO_2 , then α_1 will have a negative or positive sign in the equations.

Further attention is necessary during the solution for the fact that variables may take up values in different intervals in identical phases of the motion. Knowing the geometrical parameters of a

given mill, calculations were carried out between limit values determined by designing (see later, chapter 4). The above system of equations can be solved numerically (using e.g. gradient method).

3.3. Determining the velocity of the impact point (v_b)

After determining the position (Ω_c) and angle (φ_c) of impact in the previous point, the two components of the absolute velocity of the point, v_{bx} and v_{by}, can be calculated in the impact point 'B', within the *X* – *Y* co-ordinate system. The velocity of the impact point (v_b) at point 'B' is given by the sum of the peripheral velocity of the sun disk (v_{bp}) and the peripheral velocity of the vial (v_{bv}).

Based on the indications in Fig. 6., the peripheral velocity resulting from the rotation of the vial, and its *X*- and *Y*-direction components are:

$$v_{bv} = r_v \cdot \omega_v, \tag{3.6}$$

$$v_{bvx} = v_{bv} \cdot \cos\left(\frac{\pi}{2} - (\Omega_c - \varphi_c)\right) = r_v \cdot \omega_v \cdot \sin(\Omega_c - \varphi_c), \tag{3.7}$$

$$v_{bvy} = -\left[v_{bv} \cdot \sin\left(\frac{\pi}{2} - (\Omega_c - \varphi_c)\right)\right] = -\left[r_v \cdot \omega_v \cdot \cos(\Omega_c - \varphi_c)\right]. \tag{3.8}$$

Similarly, *X*- and *Y*-direction components resulting from the peripheral velocity of the sun disk can also be stated:

$$v_{bp} = \overline{OB} \cdot \omega_p, \tag{3.9}$$

where, *OB* is the distance between the centre of the sun disk and the point of impact 'B':

$$\overline{OB} = \sqrt{r_p^2 + r_v^2 - 2 \cdot r_p \cdot r_v \cdot \cos(\pi - \varphi_c)}, \tag{3.10}$$

$$v_{bpx} = -\left[v_{bp} \cdot \cos\left((\Omega_c - \alpha) - \frac{\pi}{2}\right)\right] = -\left[\overline{OB} \cdot \omega_p \cdot \sin(\Omega_c - \alpha)\right], \tag{3.11}$$

$$v_{bpy} = -\left[v_{bp} \cdot \sin\left((\Omega_c - \alpha) - \frac{\pi}{2}\right)\right] = \overline{OB} \cdot \omega_p \cdot \sin(\Omega_c - \alpha), \tag{3.12}$$

The sign of v_{bpx} (3.11) is negative in all cases. However, the sign of v_{bpy} (3.12) is positive if the point of impact falls to the right from the *Y*-axis of the absolute co-ordinate system, and it is negative, if it falls to the left.

Based on these the *X*- and *Y*-direction projections of the velocity of the impact point can be stated:

$$v_{bx} = v_{bvx} + v_{bpx}, \tag{3.13}$$

$$v_{bx} = r_v \cdot \omega_v \cdot \sin(\Omega_c - \varphi_c) - \overline{OB} \cdot \omega_p \cdot \sin(\Omega_c - \alpha), \tag{3.14}$$

$$v_{by} = v_{bvy} + v_{bpy}, \tag{3.15}$$

$$v_{by} = -r_v \cdot \omega_v \cdot \cos(\Omega_c - \varphi_c) + \overline{OB} \cdot \omega_p \cdot \cos(\Omega_c - \alpha). \tag{3.16}$$

The velocity components v_{ix} and v_{iy} of the absolute impact velocity are the difference between the detachment velocity (2.12, 2.14) and the corresponding velocity components of the impact point (3.14, 3.16):

$$v_{ix} = v_{dx} - v_{bx}, \tag{3.17}$$

$$v_{iy} = v_{dy} - v_{by}, \tag{3.18}$$

$$v_i = \sqrt{v_{ix}^2 + v_{iy}^2}. \tag{3.19}$$

3.4. Determining the impact energy (E_b) and the milling power (P)

In order to determine the kinetic energy of the ball, i.e. the impact energy, the normal direction component of the absolute impact velocity needs to be determined. The angle, where the impact of the ball is on the wall of the vial (φ_c), determines the amount of energy that can be transferred to the powder particles on the wall of the vial by the ball. The effective impact velocity generating the impact energy is the normal direction component of the impact velocity, broken up into the radius direction of the vial. With the marks used in Fig. 7. the normal direction component can be calculated using the relationship

$$v_{in} = v_{ix} \cdot \cos\lambda + v_{iy} \cdot \sin\lambda \tag{3.20}$$

and the tangent direction velocity component with the relationship

$$v_{it} = -v_{ix} \cdot \sin\lambda + v_{iy} \cdot \cos\lambda, \tag{3.21}$$

where λ is the angle demonstrated on Fig. 7.

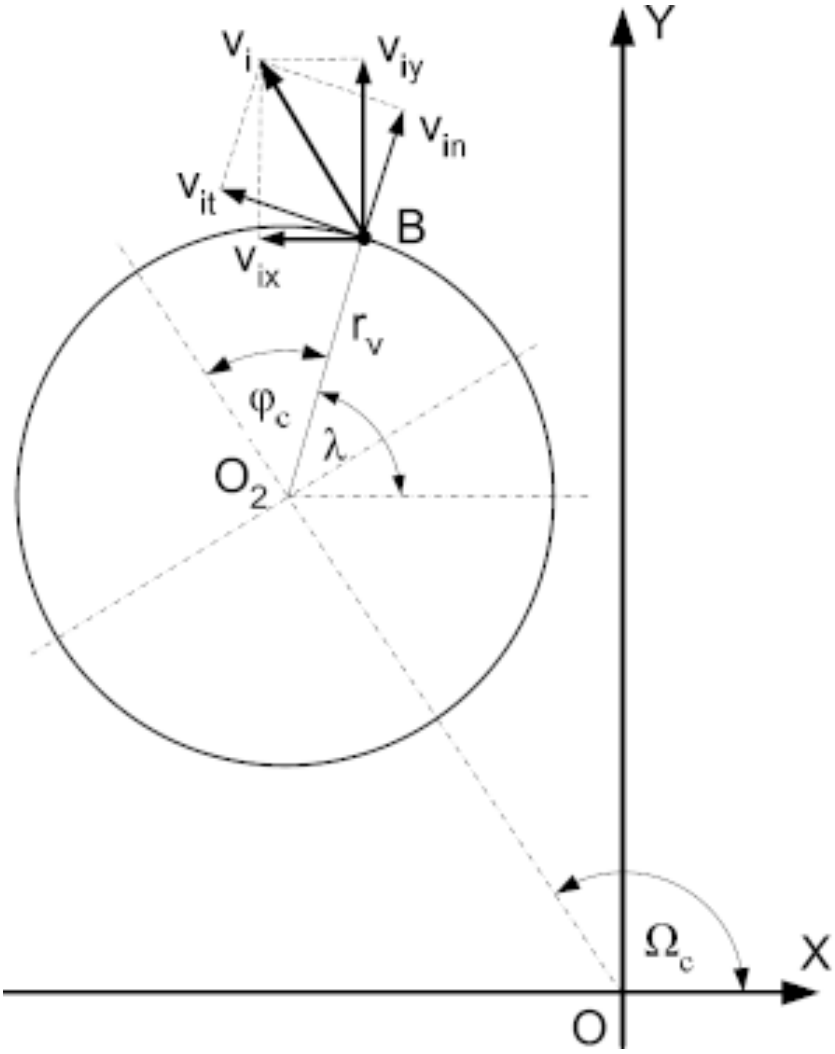

Fig. 7. Interpretation of the normal and tangential direction components of the absolute impact velocity.

After determining the above, the effective impact energy released at one single collision during the mechanical milling process can be calculated as follows:

$$E_b = \frac{1}{2} \cdot m_b \cdot v_{in}^2, \qquad (3.22)$$

where m_b: is the mass of the milling ball [kg]
v_{in}: is the effective impact velocity [m/s]
E_b: is the impact energy released at the collision [J].

The energy determined using the relationship (3.22) is transferred from the milling balls to the powder particles as many times as the balls hit the wall of the vial. The impact frequency is the number of times the ball hits the vial in one second. Knowing the total period of time the time passing between the first and the second detachment should be known in order to calculate the frequency of the impacts. Each cycle can be broken down to two periods: T_1 is the period of time during which the ball gets from the first detachment point to the first impact, and T_2 is the period of time from the first impact until the second detachment. T_1 can be calculated from (3.1), and T_2 can be determined based on the following relationship [12]:

$$T_2 = \frac{\varphi_d - \varphi_c}{\omega_v} \qquad [s]. \qquad (3.23)$$

Since the period time of the cycle is the sum of T_1 and T_2, the impact frequency f_b can be calculated. The impact frequency actually in this case means the number of impacts per second.

$$f_b = \frac{1}{T_1 + T_2} \qquad \left[s^{-1}\right]. \tag{3.24}$$

This impact frequency corresponds with the impact of the single ball in the vial. Taking the fact into consideration that in practice milling is not carried out using one ball, that is taking the number of balls in the vial into consideration, the effective impact frequency f_{eff} can be determined. However, it is supposed that there are few balls in the vial to hinder the movement of each other.

$$f_{eff} = f_b \cdot N_b \qquad \left[s^{-1}\right], \tag{3.25}$$

where N_b: is the number of balls in the vial.

Knowing the energy released by the impact (E_b) and the effective impact frequency (f_{eff}), the power of the milling process (P) can be determined:

$$P = f_{eff} \cdot E_b \qquad [W]. \tag{3.26}$$

The above described power may be suitable for comparing millings carried out using different impact energies. Greater power means that shorter milling time is necessary for the milling process.

Considering the fact that the milling is carried out to a determined time (t) on the powder having a given mass (m_p), we can define a cumulative kinetic energy (E_{kum}) normalized to the weight:

$$E_{kum} = \frac{E_b \cdot f_{eff} \cdot t}{m_p} \qquad \left[J/g, Wh/g\right], \tag{3.27}$$

where E_b: is the impact energy released at the collision [J]

f_{eff}: is the effective impact frequency [s^{-1}]

t: is the milling time [s or h]

m_p: is the mass of the powder [g].

Based on the calculation method introduced in this chapter, the impact energy of the ball and the impact frequency of the ball can be calculated, and it is apparent that these can be regulated independent from each other if the milling parameters are correctly configured. By changing the number of balls the ball impact frequency (f_{eff}) can be changed, while the impact energy of the ball (E_b) does not change. On the other hand, by changing the diameter (d_b) and density (ρ_b) of the ball, the impact energy of the ball can be changed without changing the impact frequency of the ball.

Let us note again that the model described is true and valid only if $i_{limit} \le i \le i_{critical}$ is true on the rate of the rotary speeds of the sun disk and the vial (that is on the ratio (i)).

4. APPLICATION OF THE MODEL AND CALCULATION RESULTS

Using the calculation method described in chapters 3.1. and 3.2. the milling energy values of FRITSCH P4 planetary ball mill applicable for milling experiments were determined by different configuration parameters. Different sun disk rotary speed values and ratios were taken into consideration by the calculations and at the same time the inspection of the full rotary speed range of the mill was aimed at, together with the path of motion of the balls to comply with the impact and friction method, that is $i_{limit} \le i \le i_{critical}$.

Since calculations were carried out on a given mill type, certain initial parameters were given. These were mainly the features of the device:

- distance between the sun disk and the vial: r_p = 0.125 m
- sun disk rotary speed range for test: n_p = 50 – 400 rpm.

Selection of further initial values determined by us was carried out based on the equipment available for the mill:

- inner radius of the vial (80 ml): r_v = 0.0325 m
- radius of the milling ball: r_b = 0.005 m
- density of the milling ball (stainless steel): ρ_b = 7800 kg/m^3

Knowing the above determined geometrical parameters (r_p, r_v), with the relationship (2.3) even the extreme values (i_{limit}, $i_{critical}$) of the ratio (i) can be determined, which indirectly influence even the rotary speed of the vials together with the rotary speed of the sun disk, concerning the inspected range. Extreme values of the ratio (i) are:

- bottom limit: i_{limit} = 0,96
- upper limit: $i_{critical}$ = 2.96

Calculations using the model set up in point 3. were carried out using values i = 1; 1.5; 2; 2.5; 2.96.

In the first part of the calculations, that is by the determination of the detachment angle and the detachment velocity it was found that in case of fixed geometrical conditions (r_p, r_v, r_b) and ratio (i) identical detachment angle values belong to an increasing sun disk rotational speed, while the value of the detachment velocity increases in ratio with the rotational speed of the sun disk.

After calculating the impact angle and velocity, the theoretical impact energy values belonging to the different sun disk rotational speed values were determined using the relationships of the previous subsection, for a single ball. The calculation results are shown on Fig. 8.

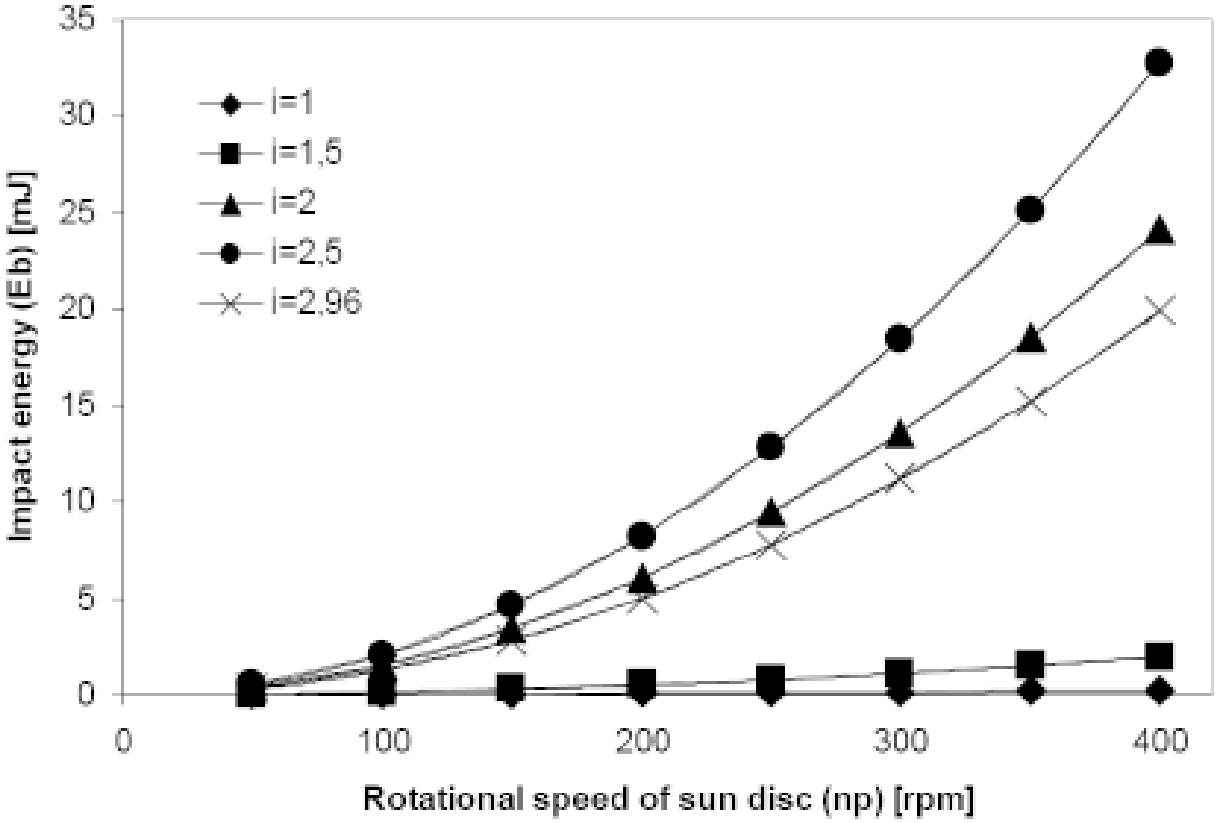

Fig. 8. Change of the impact energy (E_b) as a function of the sun disk rotational speed (n_p) and the ratio (i).

It can be seen in Fig. 8 that by increasing the rotational speed of the sun disk, the value of the impact energy increases squared up to a certain ratio. It can be seen that by i=2.96 speed ratio the curve of the impact energy is between the curves i=1.5 and i=2. This results in that probably there is an optimal value between the values i=2 and i=2.96, where the impact energy is the greatest possible. This assumption is verified by the set of curves shown on Fig. 9. The curves indicate the change of the impact energy by increasing the ratio, belonging to different rotary speed values of the sun disk. Looking at the diagram it can be found that by given geometrical conditions and configured parameters, the greatest impact energy can be achieved by approximately i=2.5. If the impact frequency of the balls can also be taken into account, which is mainly the function of the detachment and impact angles, then using the relationship (3.26) the power of the milling process can be determined.

When inspecting theoretical power values belonging to different sun disk rotational speed values and velocity rates (Fig. 10.), it can be found that greater and greater power values belong to increasing rotary speed values. The curves calculated are cubic ones.

In opposition to the changes of the impact energy shown in Fig. 8., it can be observed in Fig. 10. that the values of the curve belonging to i=2.5 are lower than those belonging to i=2 and i=2.96. The result is surprising as lower power belongs to a velocity ratio causing the greatest impact energy. This can be explained by the fact that in the case of this ratio (i=2.5) the impact frequency is lower, that is the balls spend more time on the wall of the vial.

If the milling power is represented as a function of the ratio, at different sun disk rotary speed values (Fig. 11.), then the optimum velocity rate from the aspect of milling power can be determined; in Fig. 11 this is around the value i=2.96.

Using Fig. 9 and Fig. 11 such an optimum range of ratio can be highlighted, which is maximal from the aspect of both the impact energy, and the milling power. This range, by the above determined geometrical parameters, is without doubt near i=2.

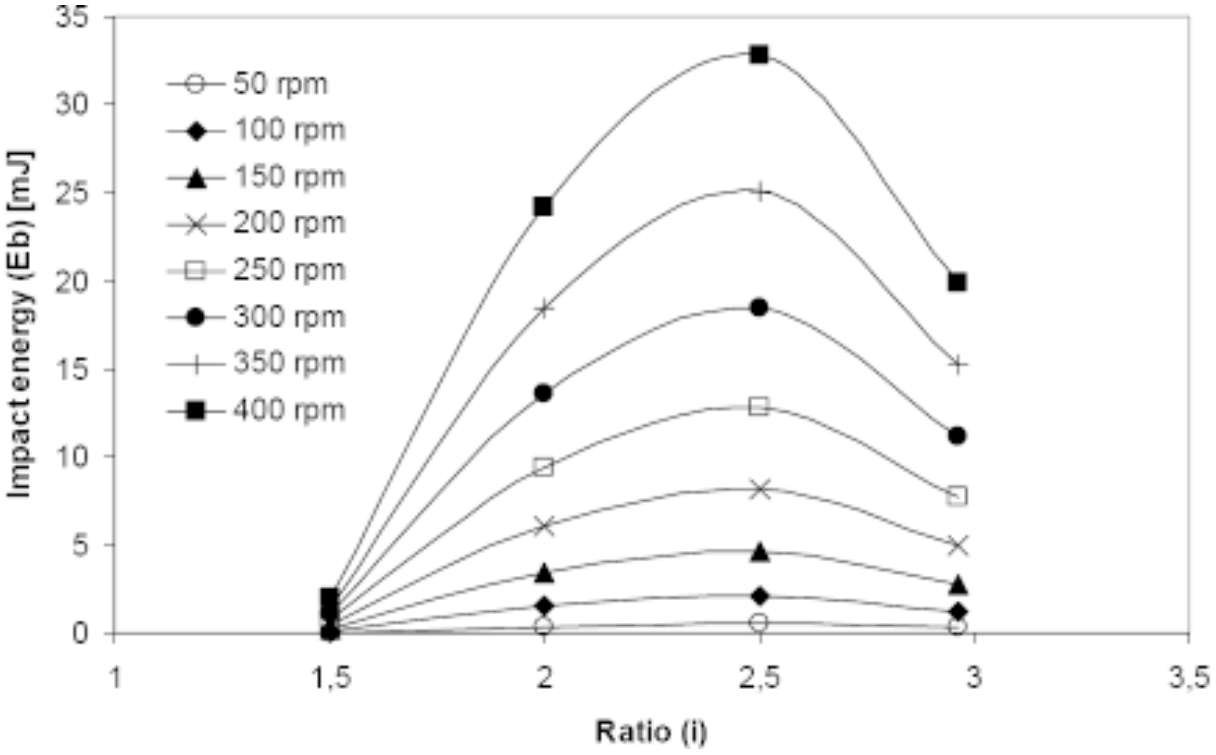

Fig. 9. Changes of the impact energy (E_b) as a function ($E_b(i)$) of increasing the ratio (i) by different rotational speeds values (i_p).

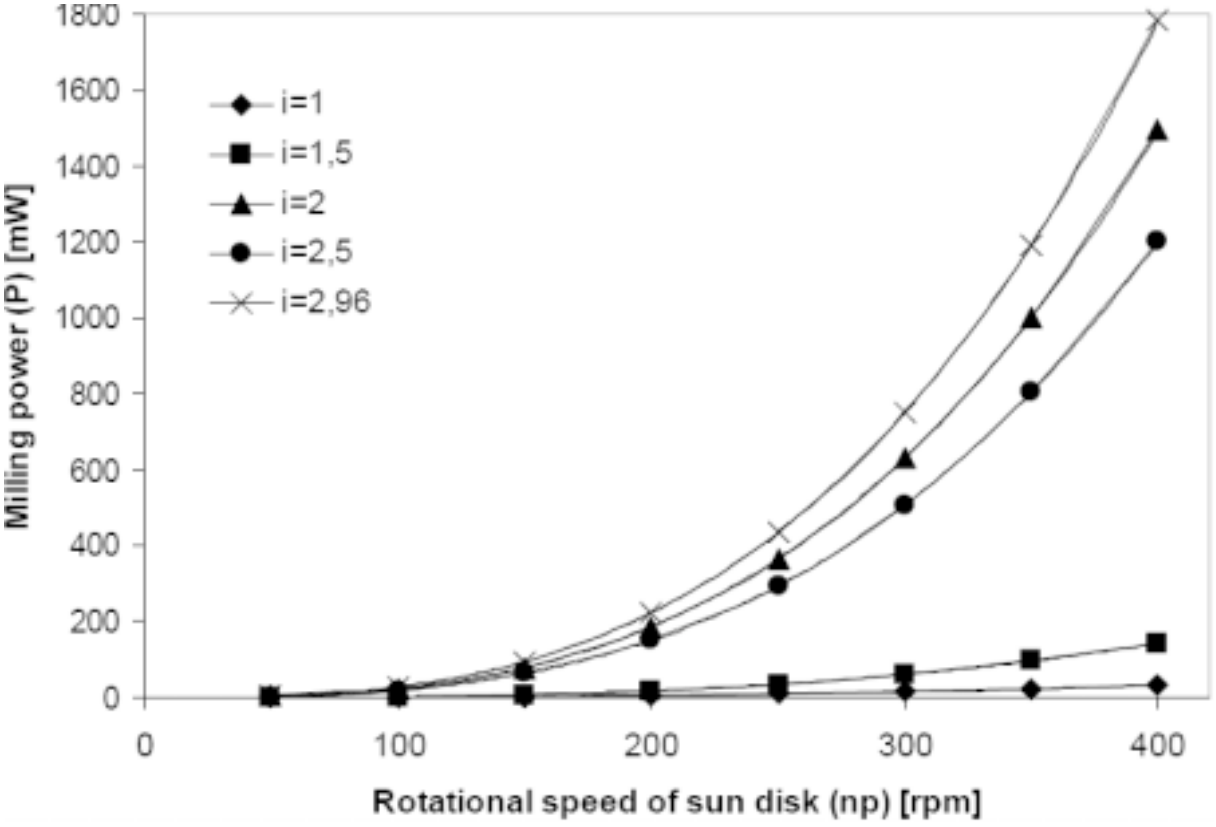

Fig. 10. Changes of the milling power (P) as a function ($P(n_p)$) of the sun disk rotational speed (n_p) and the ratio (i).

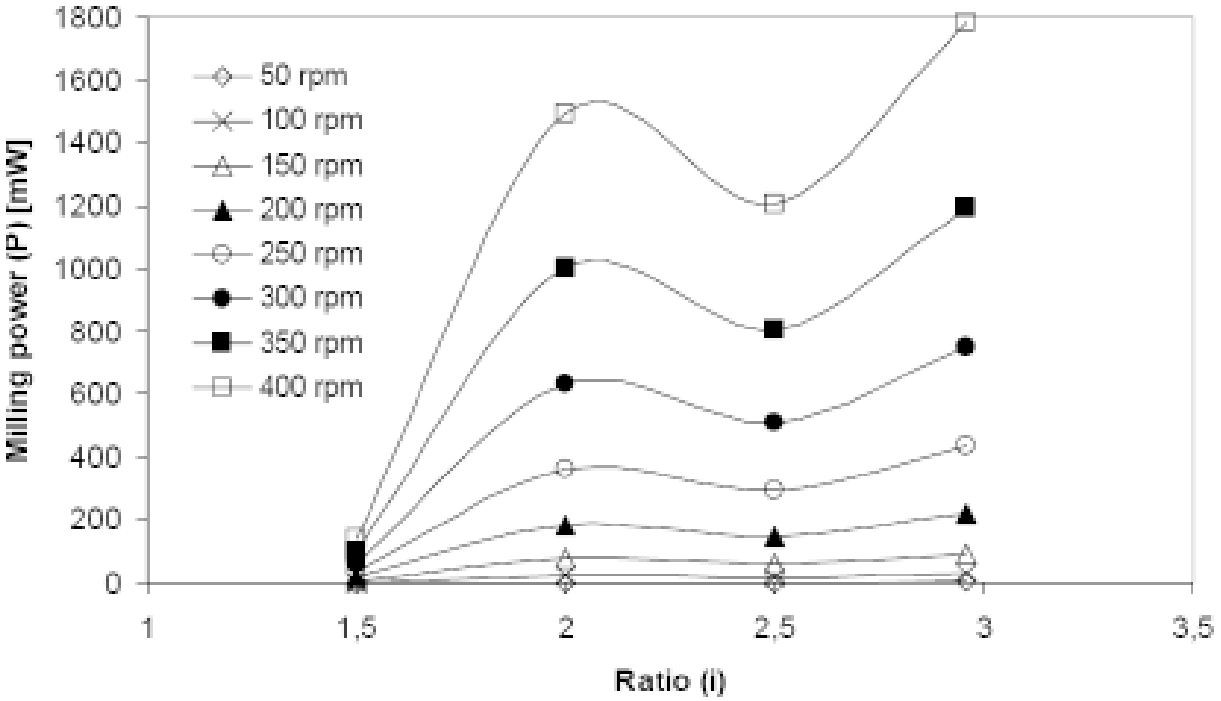

Fig. 11. Changes of the milling power (*P*) as a function (*P*(*i*)) of increasing the ratio (*i*) at different sun disk rotational speed values (n_p).

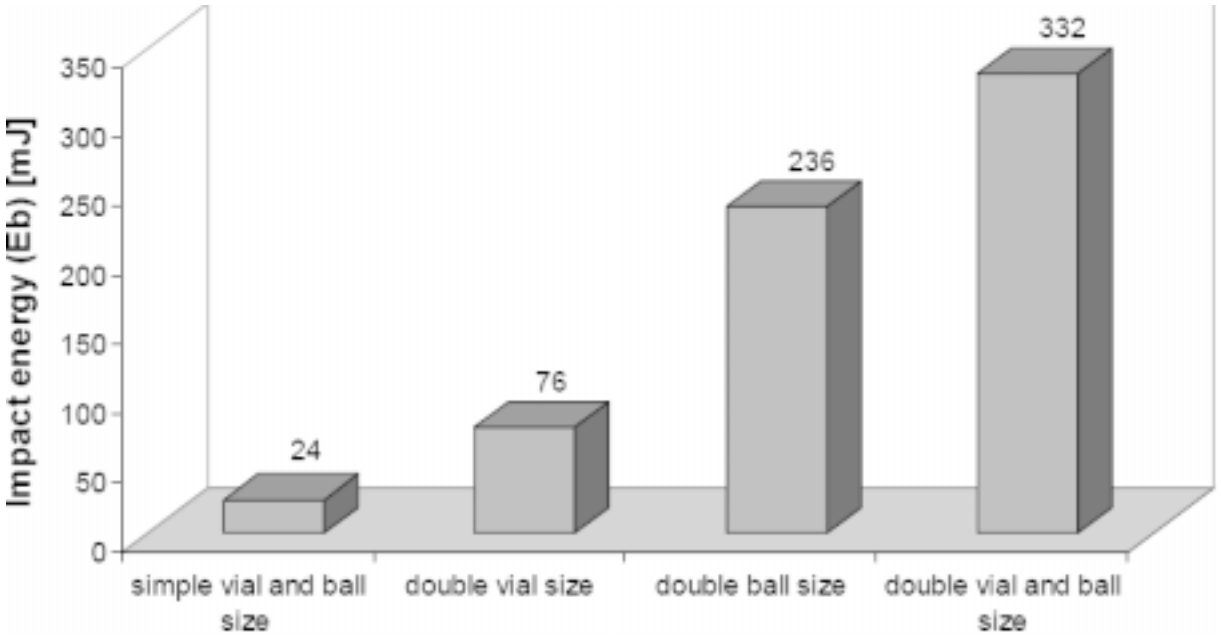

Fig. 12. Development of the impact energy due to the changes of the ball size and the vial size.

The calculation results (charts) of the model we have established were determined for given initial parameters, demonstrating the applicability of the method, it is still suitable in case of arbitrarily selected other configuration and geometrical parameters for characterizing the milling process in a planetary ball mill. Of courese, it is essential that the selected geometrical parameters should be like that the condition $i_{limit} \leq i \leq i_{critical}$ is always fulfilled for the speed rate range.

Effects of the size changes of the milling ball and the vial

The above described results were determined by fixed ball and vial sizes. In order to inspect the ef-

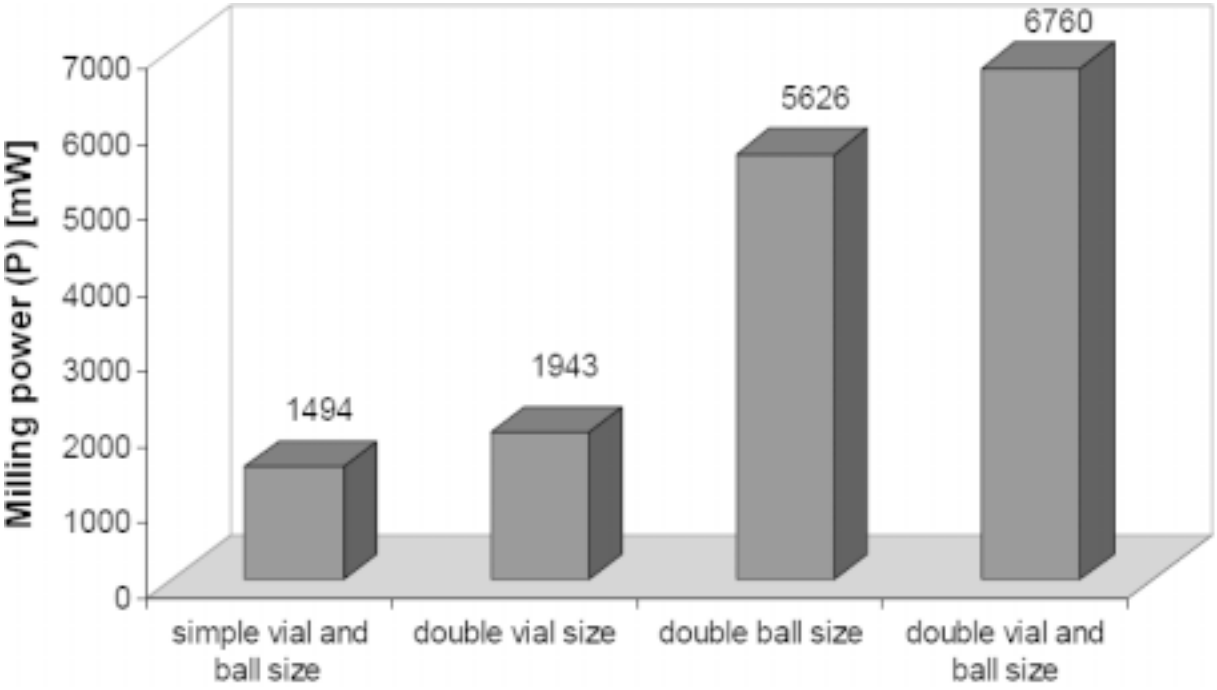

Fig. 13. Development of the milling power due to the changes of the ball and the vial.

Table 4.1. Initial parameters of the calculations inspecting the effect of the changes of the ball size and the vial size.

Studied events	Configured parameters				
	n_p [rpm]	i	r_p [m]	r_v [m]	r_b [m]
simple vial and ball size	400	2	0.125	0.0325	0.01
double ball size	400	2	0.125	0.0325	0.02
double vial size	400	2	0.125	0.065	0.01
double vial and ball size	400	2	0.125	0.065	0.02

Table 4.2. Results of the calculations inspecting the effects of ball and vial size.

	simple vial and ball size	double vial size	double ball size	double vial and ball size
Impact energy [mJ]	24	76	236	332
Impact energy increase in per cent [%]	100	315	978	1375
Milling power [mW]	1494	1943	5626	6760
Milling power increase in per cent [%]	100	130	377	452

fect of the size changes of the milling set (ball, vial) on the impact energy and power, further calculations were carried out.

First only the size changes of the vial were inspected by the same ball size, then the size of the ball was increased, and the size of the vial remained

unchanged, and finally, both the ball size and the vial size were doubled. The main initial parameters of the calculations are summarized in Table 4.1.

The diagram showing the changes of the impact energy are illustrated in Fig. 12. It can be seen in Fig. 12 that the calculation results well demonstrate and reflect the immpact energy increase expected. The results show that the increase in the vial size does not have such an effect on the increase of the impact energy, as the change of the ball size. By increasing the size of the milling set (ball, vial) together results in the greatest impact energy.

The change of the milling power has a slightly smaller increase (Fig. 13). Studying Fig. 13 it can be stated that increasing the dimensions of the milling set undoubtedly results in the increase of the milling power, however, this change is not of such degree as in case of increasing the impact energy. This is even proved by Table 4.2 comparing the calculation results.

5. SUMMARY

A calculation method was introduced above on determining the performance of a planetary ball mill. In chapter 2 the calculations of Lü and Lai [11] were used as a starting point. In chapter 3, starting from determining the impact location of the balls we have departed from the original (Lü and Lai) model, and using our own calculations the impact location and velocity of the milling ball was determined, and from these the milling energy and power were found out. From the calculated data and diagrams, in case of a given milling task the optimal milling parameters can be highlighted, which make effective work possible. Although, calculation results described in chapter 4 were determined and shown on a certain type of mill (Fritsch Pulverisette 4) and given geometrical conditions, but the model can be used for any planetary ball mill, observing the marginal conditions we have also indicated.

As a summary, it can be stated on the effect of the sizes of the milling ball and the vial on the impact energy and power, that if further milling sets are available, then using those may help gain further energy from our planetary ball mill (by the same sun disk rotary speed and ratio), increasing the efficiency of milling and decreasing the time of milling.

Based on the calculation results and the charts (Figs. 9 and 11) an optimal mill configuration can be defined, which provides for the most effective work from the aspect of the milling task. In this way, for example in case of milling certain materials, smaller impact energy can also make fast work possible, protecting the milling set and the loading of the mill.

ACKNOWLEDGEMENT

This work was supported by OTKA grants K 73776 in Hungary.

REFERENCES

[1] C. Suryanarayana, *Non-Equilibrium Processing of Materials* (Pergamon Press, Amsterdam, 1999).
[2] C.C. Koch // *Nanostructured Materials* **2** (1993) 109.
[3] J.S. Benjamin // *Scientific American* **234** (1976) 40.
[4] P.S. Gilman and J.S. Benjamin // *Annual Review of Materials Science* **13** (1983) 279.
[5] B.S. Murty and S. Ranganathan // *International Materials Reviews* **43** (1998) 101.
[6] T.H. Courtney // *Mater. Trans. JIM* **36** (1995) 110.
[7] T.H. Courtney and D. Maurice // *Scripta Mater.* **34** (1996) 5.
[8] Gy. Kakuk, A. Csanady and I. Zsoldos // *Materials Science Forum* **589** (2008) 397.
[9] P.Le Brun et al. // *Materials Science and Engineering A* **161** (1993) 75.
[10] J. Raasch // *Chemical Engineering & Tecnology* **15** (1992) 245.
[11] M. Abdellaoui and E. Gaffet // *Acta Metall. Mater.* **43** (1995) 1087.
[12] L. Lü and M.O. Lai, *Mechanical Alloying* (Kluwer Academic Publishers, Massachusetts, 1998) p. 273.
[13] N. Burgio, A. Iasonna, M. Magini, S. Martelli and F. Padella // *Il Nuovo Cimento* **13** (1991) 459.
[14] M. Abdellaoui and E. Gaffet // *Journal of Alloys and Compounds* **209** (1994) 351.
[15] M. Magini, A. Iasonna and F. Padella // *Sripta Mater.* **34** (1996) 13.
[16] M. Magini and A. Iasonna // *Mater. Trans. JIM* **36** (1995) 123.
[17] A. Iasonna and M. Magini // *Acta Mater.* **44** (1996) 1109.
[18] T. Rojac, M. Kosec, B. Malič and J. Holc, // *Journal of the European Ceramic Society* **26** (2006) 3711.

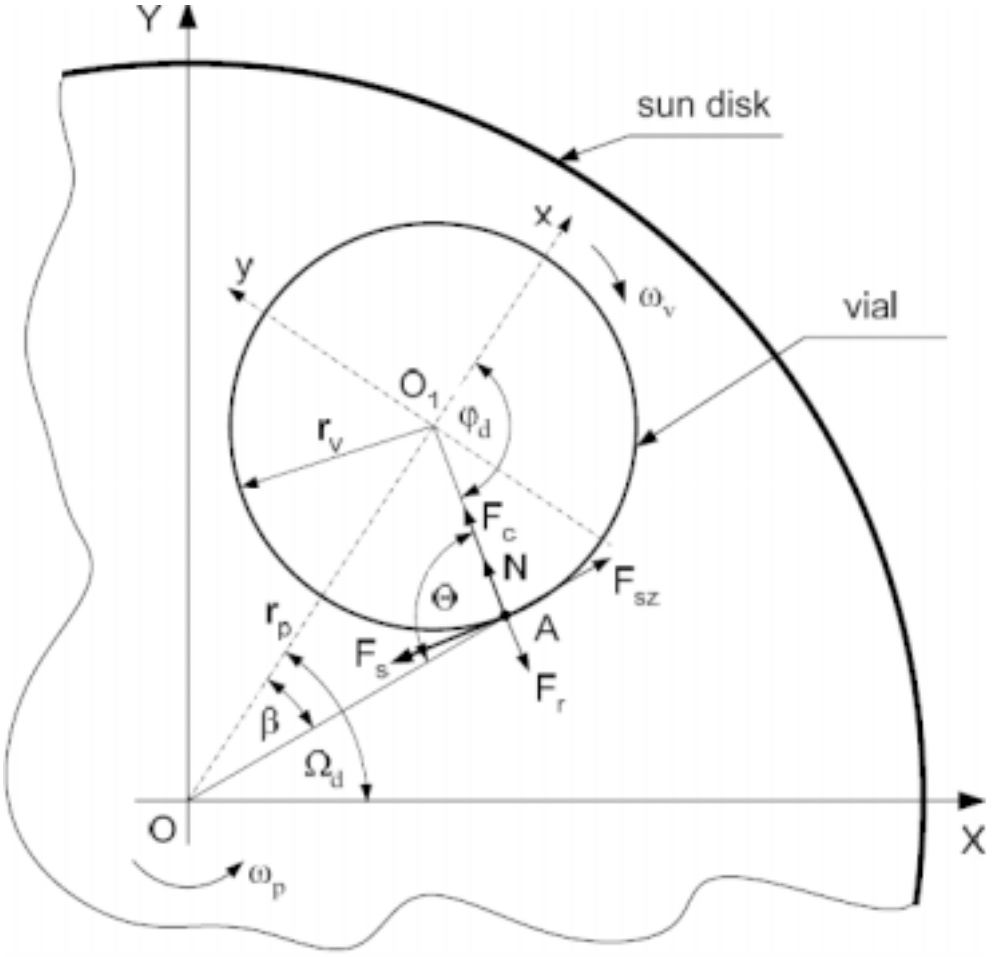

Fig. A1. Force and motion conditions in a planetary ball mill.

APPENDIX

A1. Planetary ball mill motion and force conditions.

The vial within a ball mill carries out planetary motion. The two (or in some cases four) vials with radius r_v are located on the sun disk at a constant distance of r_p from point O, around which they rotate with an angle velocity ω_p, as it is shown on Fig. A1. The centre point of the vials is point O_1, and they rotate with an angular velocity ω_v around their own axes, in the opposite direction against rotation ω_p. In the mathematical equation below, the expressions “absolute” and “relative” relate to the parameters, which were determined according to the XOY absolute and xO_1y relative co-ordinate systems. Consequently, the motion of the ball with a mass m_b along the wall of the vial can be presented as follows.

Forces acting upon the ball in the vial are the transporting force, relative force, which act from the centre of the sun disk and from the centre of the vial, marked F_{sz} and F_r. Constraining forces are N and F_s, normal and friction force, which result from the interaction of the ball and the vial, and the force F_c resulting from the Coriolis effect, and the force of gravity. Applying the D’Alembert principle the balls can be described using statical equilibrium equations, if the accelerations are taken into calculation as inertia forces, which are equal to the product of the mass of the ball and the acceleration values. Consequently, the force acting outwards from O is transporting force, the force acting outwards from O_1 is relative force, and the Coriolis force acting towards O_1 can be stated as follows:

$$\vec{F}_{sz} = -m_b \cdot \vec{a}_{sz}, \tag{A.1}$$

$$\vec{F}_r = -m_b \cdot \vec{a}_r, \tag{A.2}$$

$$\vec{F}_c = -m_b \cdot \vec{a}_c, \tag{A.3}$$

where m_b is the mass of the ball, a_{sz}, a_r and a_c are the transportation acceleration from O, relative acceleration from O_1, and the Coriolis acceleration. Acceleration values can be stated as follows:

$$\vec{a}_{sz} = \vec{\omega}_p \times \vec{v}_p, \tag{A.4}$$

$$a_{sz} = \overline{OA} \cdot \omega_p^2 = \frac{r_p + r_v \cdot \cos\varphi_d}{\cos\beta} \cdot \omega_p^2, \tag{A.5}$$

where φ_d is the angle of detachment of the ball from the wall of the vial, Fig. A1.

$$\vec{a}_r = \vec{\omega}_v \times \vec{v}_v, \tag{A.6}$$

$$a_r = r_v \cdot \omega_v^2 \tag{A.7}$$

and

$$\vec{a}_c = 2\vec{\omega}_p \times \vec{v}_v, \tag{A.8}$$

$$a_c = 2 \cdot \omega_p \cdot \omega_v \cdot r_v. \tag{A.9}$$

The resultant of forces within the system can be stated according to Fig. A1:

$$\sum \vec{F} = m_b \cdot (\vec{a}_{sz} + \vec{a}_r + \vec{a}_c), \tag{A.10}$$

$$N = F_r - F_c - F_{sz} \cdot \cos(\pi - \theta), \tag{A.11}$$

where N is the normal force acting upon the surface of the vial, which is the inertia force resulting from the acceleration of the ball.

Using Eqs. (A.5), (A.7), and (A.9) the forces can be stated as:

$$F_{sz} \cdot \cos(\pi - \theta) = m_b \cdot a_{sz} \cdot \cos(\pi - \theta) = m_b \cdot \omega_p^2 \cdot \frac{r_p + r_v \cdot \cos\varphi_d}{\cos\beta} \cdot \cos(\pi - \theta), \tag{A.12}$$

$$F_r = m_b \cdot r_v \cdot \omega_v^2, \tag{A.13}$$

$$F_c = 2 \cdot m_b \cdot \omega_p \cdot \omega_v \cdot r_v. \tag{A.14}$$

A2. Determining the detachment angle of the milling ball.

Let us suppose that when *N=0* the ball detaches from the surface of the vial wall. This crucial condition can be stated as follows:

$$N = 0, \tag{A.15}$$

$$m_b \cdot \omega_p^2 \cdot \frac{r_p + r_v \cdot \cos\varphi_d}{\cos\beta} \cdot \cos(\pi - \theta) + 2 \cdot m_b \cdot r_v \cdot \omega_p \cdot \omega_v = m_b \cdot r_v \cdot \omega_v^2. \tag{A.16}$$

Let the relationship (ratio) between the angular velocity of the vial and the sun disk will be as follows:

$$i = \frac{\omega_v}{\omega_p}. \tag{A.17}$$

Settling Eq. (A.16) and after carrying out the appropriate modifications, and using Eq. (A.17) the angle of detachment of the ball from the wall of the vial can be determined [12].

If the sun disk rotates anticlockwise while the vial rotates clockwise, the angle of detachment will be as below:

$$\varphi_d = \arccos\left(-\frac{r_v \cdot (1-i)^2}{r_p} \right). \tag{A.18}$$